

DOI: <https://dx.doi.org/10.21123/bsj.2023.7204>

The Influence of Ablation Speed on the Synthesis of Carbon Nanostructures Via Pulsed Laser Ablation of Asphalt in Ethanol

Huda Mahmood Al-attar^{1*} 

Mohanad Mousa Azzawi² 

¹ College of Engineering, University of Baghdad, Iraq

² Laser and Electro-Optic Research center, Ministry of Science and Technology, Baghdad, Iraq

*Corresponding author: huda.al-attar@coeng.uobaghdad.edu.iq

E-mail addresses: mohanad_1965@yahoo.com

Received 17/3/2022, Revised 6/8/2022, Accepted 7/8/2022, Published Online First 20/2/2023,
Published 1/10/2023



This work is licensed under a [Creative Commons Attribution 4.0 International License](https://creativecommons.org/licenses/by/4.0/).

Abstract:

Pulsed liquid laser ablation is considered a green method for the synthesis of nanostructures because there are no byproducts formed after the ablation. In this paper, a fiber laser of wavelength 1.064 μm , peak power of 1 mJ, pulse duration of 120 ns, and repetition rate of 20 kHz, was used to produce carbon nanostructures including carbon nanospheres and carbon nanorods from the ablation of asphalt in ethanol at ablation speeds of (100, 75, 50, 10 mm/s). The morphology, composition and optical properties of the synthesized samples were studied experimentally using FESEM, HRTEM, EDS, and UV-vis spectrophotometer. Results showed that the band gap energy decreased with decreasing the ablation speed (increasing the ablation time), the minimum mean particle size of the synthesized samples was 76 nm at an ablation speed of 100mm/s, while the maximum mean particle size was 98 nm at ablation speed of 50 mm/s, the nanospheres were agglomerated to form larger spherical nanoshapes. All the synthesized carbon nano colloids exhibited a blue-green PL emission. It was concluded that the presence of carbon nanorods has an effect on the optical properties of the synthesized nanospheres.

Keywords: Carbon nanorods, Carbon nanospheres, Fiber Laser 1.06 μm , Photoluminescence, Pulsed Laser Ablation.

Introduction:

Carbon based materials include, carbon nanotubes, Graphene, carbon nanodots, fullerene, carbon fibers, and nanodiamonds^{1, 2}, which have played a vital role in developing a new class of quantum electronic devices, in medicine and in water purification due to their outstanding electrical, mechanical, physical, chemical and optical properties²⁻⁴.

In the last decade, various nanostructures were prepared efficiently by pulsed laser ablation of a solid target in liquid media. Laser ablation is considered an efficient way to prepare Carbon Quantum Dots (CQDs) with narrow size distribution, high purity, strong fluorescent characteristics, and easiness, fast, inexpensive and friendly to the environment.^{4, 5} Nevertheless, this method suffers from difficulty in controlling the stability and particle size.⁶ The morphology, structure and size distribution can be changed by changing one of the laser parameters (e.g. wavelength, fluency, pulse

width) or the liquid medium (e.g. type of the liquid and its volume)⁷.

Thongpool and coworkers studied the effect of ethanol medium on physical, chemical and optical properties of carbon particles synthesized by ablation of graphite target ablated using pulsed Nd: YAG laser beam, they observed that the synthesized particles have a broad size distribution from 200-500 nm with a flower-like morphology⁴.

Zhang and his coworkers synthesized carbon/graphene QDots without any surfactant through alkaline assisted oxidation of cellulose acetate and studied their photoluminescence properties, they discovered that as the concentration of the colloid varies the luminescence properties can be changed⁸. Sadeghi and his coworkers studied the effect of changing the liquid environment on the properties of nanoparticles and graphene nanosheets by liquid ablation of graphite using pulsed Nd: YAG laser, they found that the liquid environments have a

strong effect on the size and morphology of the nanostructures⁹, Dizajghorbani and his coworkers studied the effect of ablation time and laser fluence on the composition, morphology and optical properties of the synthesized nanoparticles from Cu target in water, they observed that there is an increase in the crystallinity of the phase of Cu₂O as the laser fluence increases at a constant ablation time,⁷ While Yogesh and coworkers have studied the photoluminescence properties of post ablated water soluble nanoparticles in ethanol, he discovered that the Carbon nanoparticles exhibit wavelength-dependency upon photoluminescence emission,⁵, and there are still researchers working in this field.

In this work due to the novel properties of nanomaterials compared to bulk due to quantum confinement effect and the high surface area to volume ratio have made nanomaterials of great importance¹⁰, we have synthesized carbon nanoparticles by ablation of asphalt as a source of carbon used for the first time as far to our knowledge by fiber laser with a wavelength of 1.064 μm , Repetition Rate 20kHz, Pulse duration 120 ns, peak pulse energy 1 mJ in Ethanol as a liquid medium, using pulsed laser ablation in liquid (PLAL). It is considered a green method, so one can prepare pure well-crystallized nanoparticles without any by-products compared to other methods¹¹. Since other researchers have studied the PLAL on Graphite, Charcoal and other materials, they have studied the influence on the size, morphology and PL of the synthesized carbon nanostructures.^{2, 4, 12-14}, that's why we wanted to investigate the influence of varying the ablation speed of the laser source by 100, 75, 50, 10 mm/s on the optical, morphology and size of the synthesized particles from the asphalt as a source of carbon.

Materials and Method:

Asphalt sample from Al-Dura oil refinery with the following specifications listed in Table.1 was used as a target in this work where a sample of 2.5 cm diameter was put on the bottom of a 40 ml beaker filled with 10 mL Ethanol as a liquid medium from Sigma Aldrich with a purity of 99.9%, a fiber laser (RAYCUS, China) of wavelength 1.064 μm , single pulse energy of 1 mJ, pulse duration of 120ns, focal length of the lens of 112 mm, with an average spot Diameter of 6 mm, Repetition Rate of 20 kHz .

The power used to ablate the target was 6 Watts, the laser fluency which is energy/diameter spot area of 3.5 mJ/cm², the scanning speed was varied by 100, 75, 50, 10 mm/s where these samples were recorded as (S1-S4) as shown in Table.2

Table 1. the specifications of the Asphalt

API Gravity at 15.6 °C	Density at 15.6 °C	Carbon wt%
30.8	0.8718	5.1

Table 2. PLA parameters for the synthesized samples in Ethanol

Sample No.	S1	S2	S3	S4
Ablation Speed mm/s	100	75	50	10
Ablation time s	68	94	136	544

Characterization:

The optical absorption spectra of the synthesized colloid were recorded using a UV-visible double beam (200-1100 nm) (LABOMED.INC., USA), the photo luminescent spectra were recorded using a fluorescence spectrophotometer (CARY Eclipse, Australia), where the sample was excited within the wavelength range from 250-500 nm, the topography was recorded using Electron Microscope (HRTEM) (Zeiss Leo 912), Ab-100 KV, the morphology, the average particle size for each sample was recorded and the elemental composition of the samples was recorded using Scanning Electron Microscope (FESEM), 10 KV (Zeiss SIGMA VP) and EDS respectively.

Results and Discussion:

Morphology:

The morphology of the synthesized carbon nanostructure for the four samples S1-S4 under a scale of 1 μm is shown in Fig.1 a-d respectively. S1 has shown to be consist mainly of a dense collection of nanorods with the smallest diameter of 57 nm, while the nanospheres are agglomerated in a spherical shape attached to the rod surface due to the strong inter-atomic interaction forces between them, the attraction forces between the synthesized nanospheres and the solvent particles are weaker than those between the nanospheres themselves, and the Vander Waals forces are strong.^{13, 15}

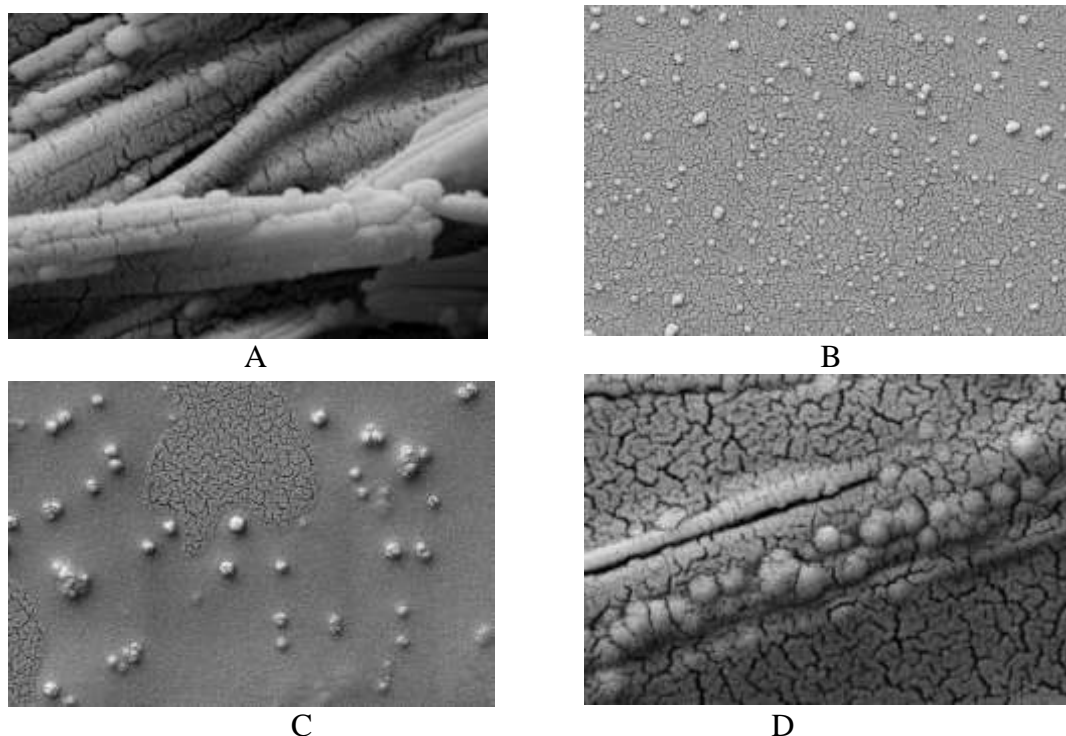


Figure 1. (a-d) SEM of the samples S1-S4 respectively, scale 1 μm .

The elemental composition was recorded by EDS. Fig.2 a shows the EDS of the asphalt, while Fig.2 b and c show the EDS of S3 and S4 samples, the presence of Au and Si is due to the fact that the synthesized colloids are deposited on a glass substrate which consists mainly of SiO_2 and the deposited film is gold coated to increase its conductivity since asphalt consists of a mixture of

complicated hydrocarbons, Fig. 2 (b) shows that the synthesized colloid consists mainly of carbon, while Fig.2 (c) EDS has shown the presence of Na and fluorine besides the carbon content, i.e. the synthesized carbon nanostructures were functionalized with fluorine and sodium forming organometallic compound due to irradiation of asphalt with the laser source for longer time.

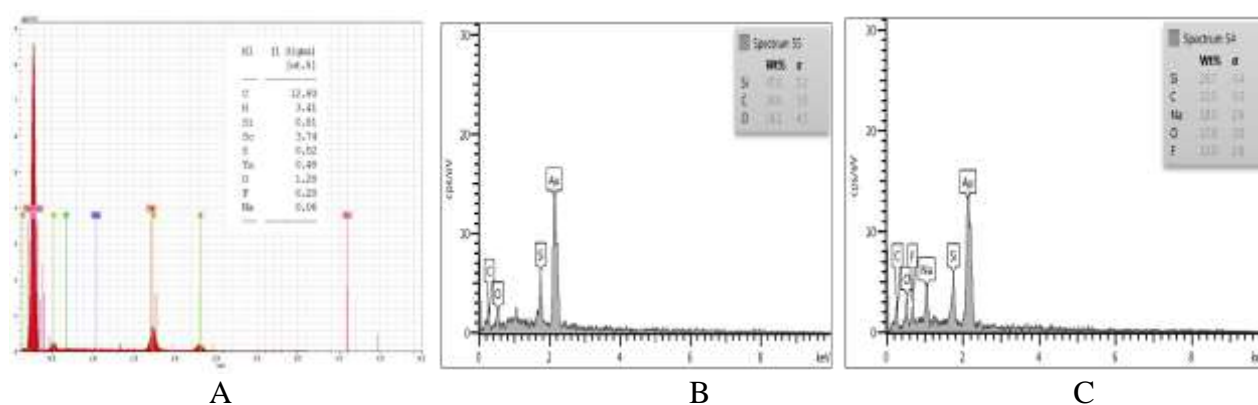


Figure 2. EDS of (a)asphalt (b) S3, (c) S4.

Fig. 3 a and b shows the TEM 2-D image of sample 3 and 4 respectively, both show a 2-D Image of the carbon nanorods with the nonuniform shapes attached on their surface, although the nanorods have not appeared in SEM image of S3, S4 consists of dense collection nanorods with different nanostructures attached to it, and the size of the nanorods has shown to be smaller in its length and

diameter than those in S3. The formation of carbon nanorods is attributed to Ostwald ripening Mechanism and this formation consists of two steps: the first step is the head to tail connection which is responsible for the assembly of nanorods from disordered nanoparticles, and the final step is the disappearance of the small nanoparticles.¹⁶

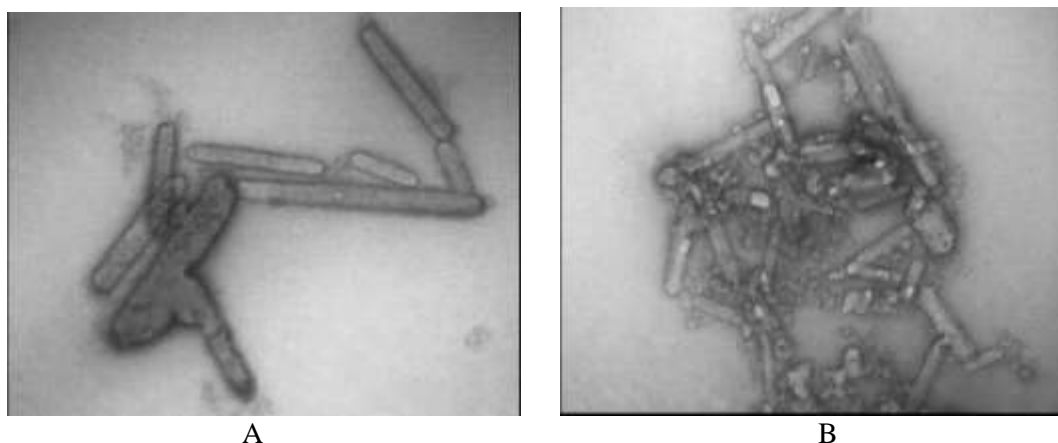


Figure 3. TEM of (a) S3, (b) S4 scale 200 nm

The particle size distribution of the carbon nanospheres of the synthesized samples S1-S4 are shown in Fig.4 a-d respectively, all the samples are a mix of nano and micro particles, the presence of agglomerated particles might be due to Ostwald ripening mechanism and the strong interatomic interaction between the nanospheres, due to the higher solubility of the crystals, Ostwald mechanism is responsible for the larger growth of crystals from smaller size particles, ¹⁶, S3 has the largest mean particle size diameter of 98 nm, and S1 has the smallest mean particle size diameter of 76 nm, due to the quantum confinement effect S1 has the smallest particle size diameter and hence the largest E_g of 4 eV, and S4 has the largest mean particle size

diameter and the smallest E_g of 3.4 eV, which can be used as a photocatalyst to degrade dyes like Methylene blue (MB) or Rhodamine B (RhB) in water,¹⁷ the presence of nanorods might have affected the value of E_g , the lower concentration of the nanoparticles is suggested for S1 and S2 which explains the low intensity peaks of UV-VIS spectrum and this coincides with the results obtained by.²

From Figs. 1, 4 the spherical shapes in S2 are the smallest compared to all samples, while the spherical shapes in S3 are larger than those in S1, also, S4 consists of few nanorods with the smallest diameter of 72 nm and the spherical shapes are also attached to the surface of the nanorods.

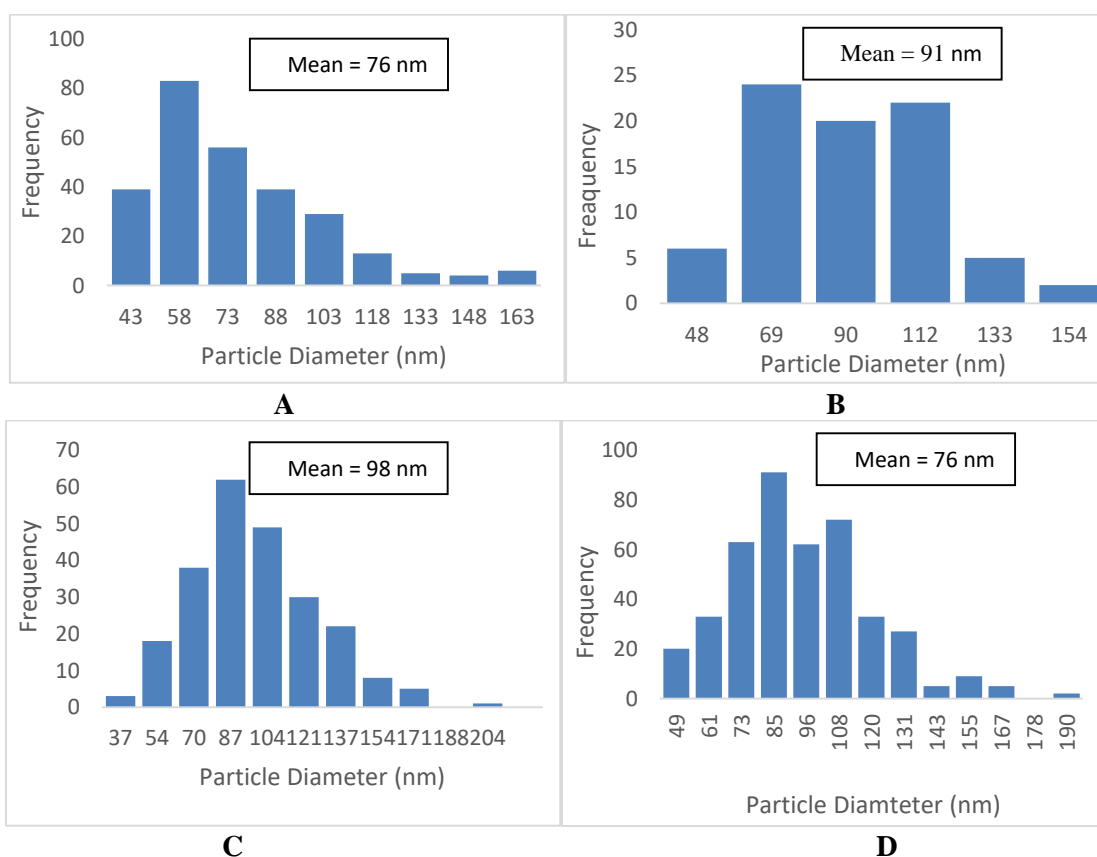


Figure 4. (a-d) The particle Size Diameter of the synthesized nanospheres of S1-S4 respectively

Optical Properties

The color of the solution is an indication of the concentration (amount of nanoparticles in ethanol) as shown in Fig.2. The color is changed from dark yellow to faint yellow for S4-S1 in accordance with ^{9, 14}.



Figure 5. The synthesized nanostructures in Ethanol S1-S4

Fig.6 shows the UV-visible absorption spectroscopy of samples (S1-S4), it is obvious that varying the ablation speed has affected the characteristics of the UV-VIS absorption peaks, by increasing the ablation time the absorption peak intensity increases which coincide with the results obtained by ^{7,6} and ¹⁸, around 230-280 nm is the typical absorbance peak of carbon nanostructure,⁵ all the samples have shown absorbance peak around 290 nm which are attributed to $\pi-\pi^*$ of C=C respectively ^{2,14}, and ¹² since more than one peak was recorded this means that there are other particles not only carbon nanoparticles were synthesized and this explains the functionalization of carbon colloid of S4 obtained by the EDS in Fig. 2 b, also lowering the ablation speed (increasing the ablation time) results in an increase of the intensity peaks i.e. broadening of FWHM, i.e. red shift towards higher values in wavelength 255, 257, 258, 260 for S1 to S4 respectively, this coincides with the results obtained by ^{7, 6, 18}, the red shift in the spectrum refers to an increase in the particle size of the sample with lowering the ablation speed (increasing the ablation time, and this

contradicts the results obtained by ⁷ and, ⁶ it seems that S3&S4 due to lowering the ablation speed the molecules of ethanol had adsorbed on the surface of the carbon nanostructures ⁴, while S1&S2 have shown the narrower excitonic peak compared to the other samples which is an indication of the narrow size distribution of the nanoparticles of the colloid in these samples, ¹¹ from the above obtained results, this confirm that uv-vis spectrum is size and concentration dependent. From Fig. 6, it is obvious that S4 has the largest broadening of FWHM among all the samples this can be justified by the functionalization shown in the EDS in Fig.2 b.

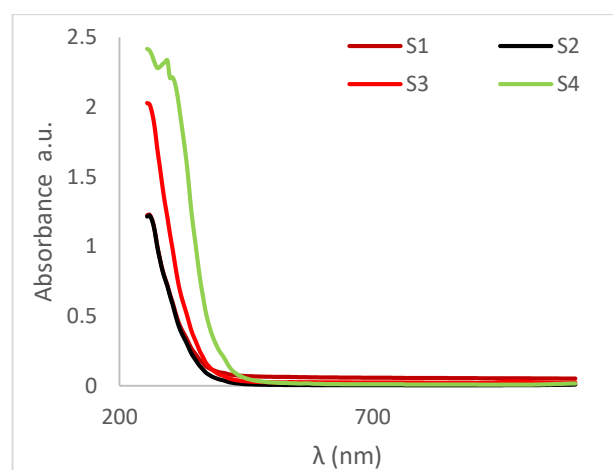


Figure 6. UV-Vis spectrum of the synthesized nanostructures in Ethanol

The optical properties of quantum sized particles can be monitored efficiently depending on the uv-visible absorption spectrum, increasing the ablation time has resulted in decreasing in the optical energy gap due to an increase in the particle size, these results coincide with the results obtained by⁷, i.e. Red shift in the absorption spectrum which is attributed to quantum confinement effect, (as confirmed by Tauc Plot in Fig.7), a list of band gap energies are shown in Table. 3, where a functionalization of the carbon nanostructures can be done to shift the energy gap to the visible region, and this can qualify the synthesized nanostructures to be used in a solar cell or in photocatalytic applications. Tauc plots were calculated using the following equation for linear allowed transition ^{19, 20}

$$(\alpha h\nu)^2 = (h\nu - E_g)$$

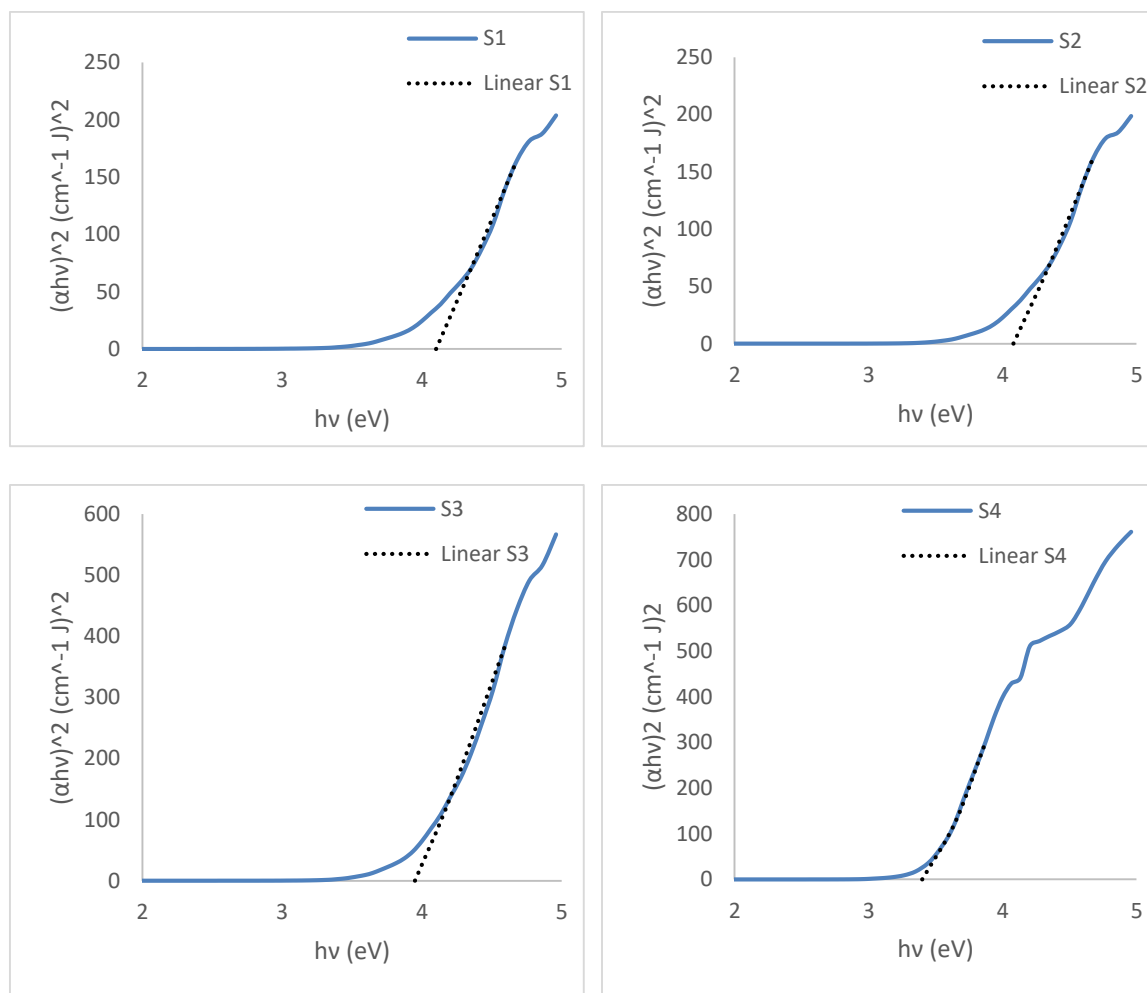


Figure 7. Tauc's plot of the synthesized samples of S1-S4 respectively

Table 3. Band gap energy of the synthesized samples using linear allowed transition

Sample No.	S1	S2	S3	S4
E_g (eV)	4.1	4.08	3.95	3.4

Fluorescence is size and concentration dependent, Fig.8, shows the PL spectrum of samples S1-S4 under an excitation wavelength of $\lambda=350$ nm, the sharp PL peak of S4 refers to band-band transition and it indicates that the synthesized sample is of high purity⁶, from the spectrum the synthesized samples can be used in the fabrication of violet LED and other optoelectronic applications and it can be used in bio imaging, It was found that the PL intensity increases with increasing the ablation time (i.e. decreasing the ablation speed), the largest particle size has the highest fluorescence intensity S4, while the smallest has the lowest intensity S1, and this justifies the results obtained in Table 3 that due to quantum confinement effect the widest energy gap has the lowest particle size,⁸ the red shift in the spectrum might be due to the adsorption of the

ethanol molecules on to the surface of the carbon nanoparticles⁴, S4 has the largest value of FWHM of 79 nm between the samples this can be attributed to the large size distribution of the particles⁸, and this coincides the results obtained by UV-visible spectrum.

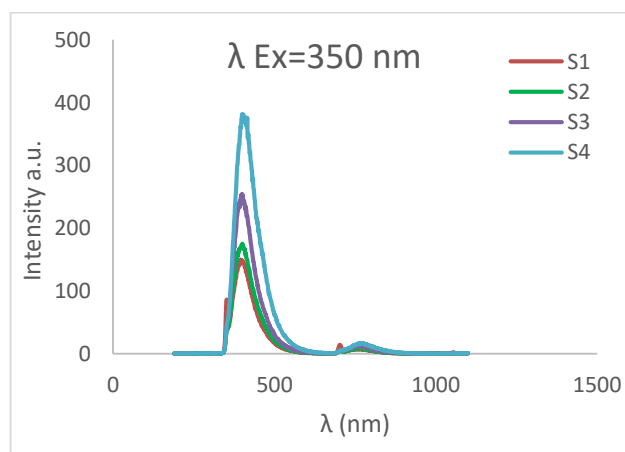


Figure 8. The PL emission for samples S1-S4 at Excitation wavelength of 350 nm

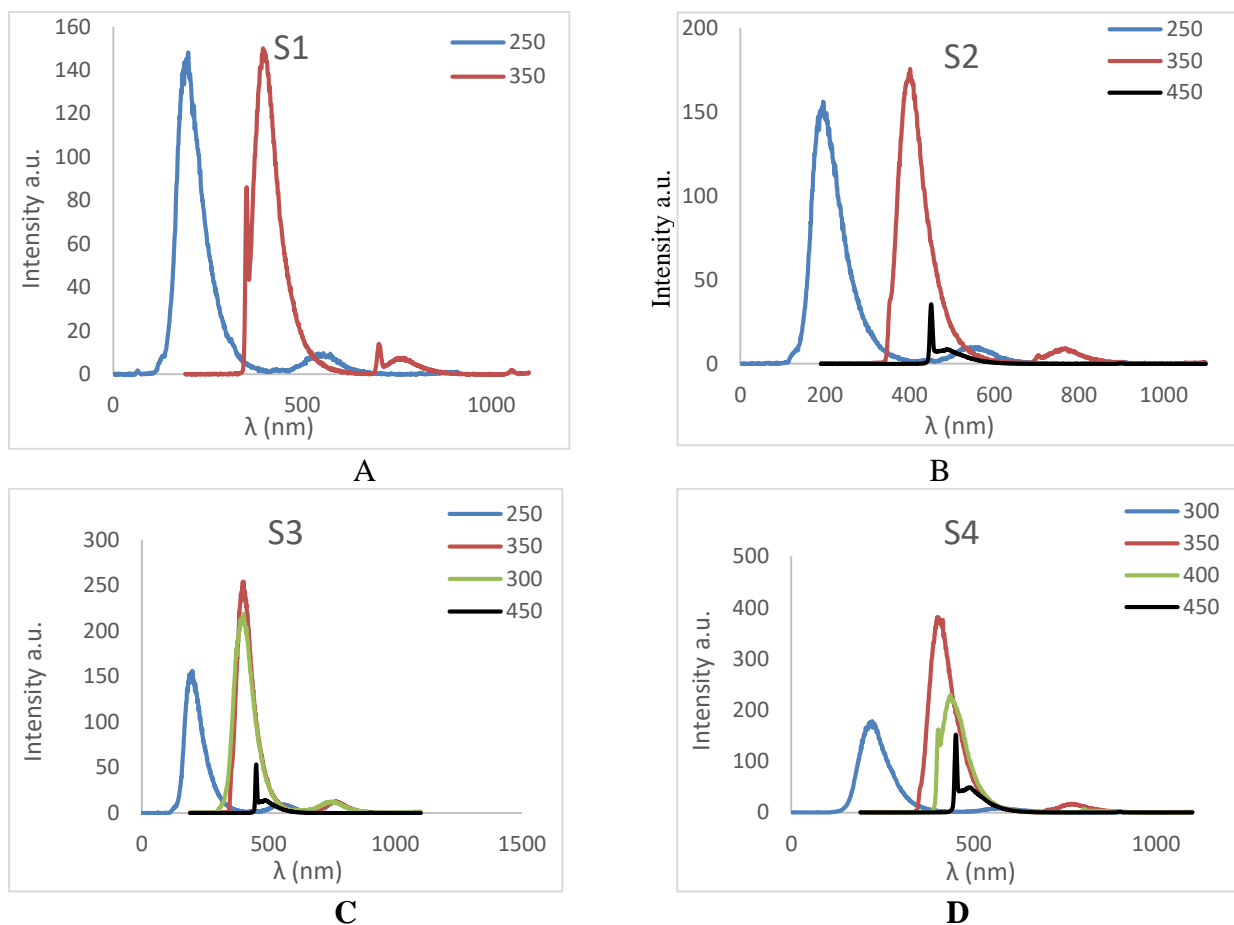


Figure 9. PL emission at different excitation wavelength for (a) S1, (b) S2, (c) S3, (d) S4

Fig.9 (a)-(d) demonstrates the PL emission spectra of the sample (S1-S4) respectively at the different excitation wavelengths, it is obvious from the above figures that all the samples exhibit a monotonic red shift with increasing excitation wavelength, in accordance with,^{8, 13} the PL spectra of all the samples is resulted from the difference in particle sizes of the samples and from the existence of different emissive sites that are called surface energy traps which have resulted in a broad spectrum and wavelength excitation dependence and multi-color PL, in accordance with,²¹⁻²³.

Fig.10 (a, b) shows the strongest emission of the samples S1-S4 as a function of wavelength and intensity respectively, from UV-vis absorption spectra S1 and S2 have the lowest concentration, while S3, and S4 have the highest, from Fig.10 (a) it is obvious that there is a blue shift in the emission wavelength with reducing the ablation time for S4-S1, this coincides the results obtained by⁸, i.e. S1 is the most diluted sample, while for the intensity there is an exponential decrease with decreasing the ablation time and this contradicts the results obtained by⁸, while more studies have to be done to understand this phenomenon.

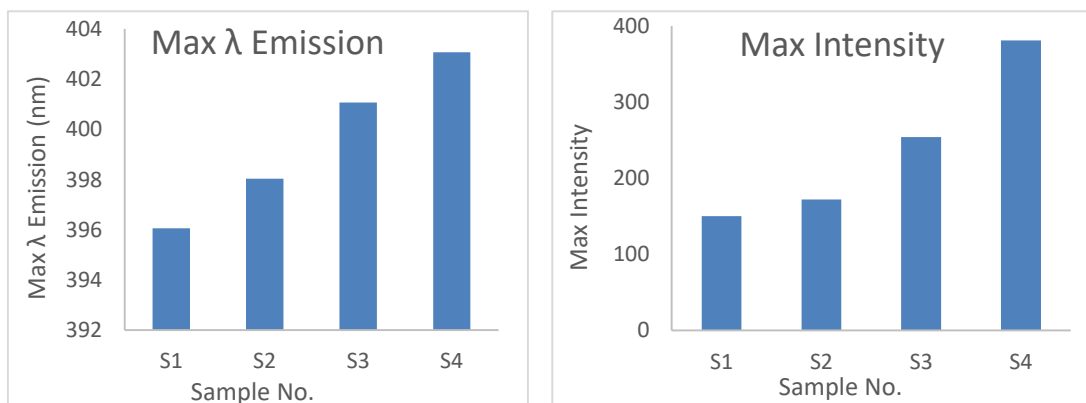


Figure 10. The strongest emission of samples S1-S4 in (a) wavelength, (b) intensity

Fig.11 shows a green blue PL emission after irradiation the samples with a laser source of wavelength 405 nm this confirms that synthesized colloid can be used in bioimaging.^{24, 25}



Figure 11. The synthesized carbon nanostructure dispersed in ethanol after irradiation with 405 nm laser beam

Conclusions:

Green synthesis of carbon nanostructures consisting of nanospheres and nanorods was successfully synthesized from the ablation of asphalt in ethanol at different ablation speeds. Increasing the ablation time (lowering the ablation speed results in smaller nanorods diameter and length. The shorter the ablation time the smaller the mean particle size diameter, the longer the ablation time the smaller, the energy gap with $E_g = 3.4$ eV is the minimum energy gap at an ablation speed of 10 mm/s, the presence of functionalized nanorods has an effect on the value of the E_g which means that the presence of nanorods has an effect on the optical properties of the synthesized carbon nanospheres. The intensity of the absorption peaks indicates that the amount of mean carbon particle size diameter is the maximum at the ablation speed of 50 mm/s, the formation of spherical shapes agglomerated from nanospheres indicates that the inter atomic forces between nanospheres are high and there is a necessity to use a capping agent to increase the stability of the synthesized colloids since the Vander Waals forces between the synthesized nanospheres are strong. The maximum fluorescence intensity was achieved at an ablation speed of 10 mm/s i.e. the longest ablation time due to the functionalization of the surface with fluorine and sodium, which result in an enhancement in the PL spectra.

Authors' declaration:

- Conflicts of Interest: None.
- We hereby confirm that all the Figures and Tables in the manuscript are mine ours. Besides, the Figures and images, which are not mine ours, have been given the permission for re-publication attached with the manuscript.
- Ethical Clearance: The project was approved by the local ethical committee in University of Baghdad.

Authors' contributions statement:

H. M. Al. writing original draft, conceptualization, analysis of data, revision. M. M. A. participated in explaining the results, participated in the experimental part, proofreading

References:

1. Wang X, Feng Y, Dong P, Huang J. A Mini Review on Carbon Quantum Dots: Preparation, Properties, and Electrocatalytic Application. *Front Chem.* 2019; 7: 1–9.
2. Sadeghi H, Solati E, Dorrnian D. Producing graphene nanosheets by pulsed laser ablation: Effects of liquid environment. *J Laser Appl.* 2019; 31: 042003.
3. Kadhim H B A, Ridha N J, Alosfur M, Umran F K, Madlol N M, Tahir R, et al. Ablation of ZnO in liquid by Nanosecond Laser. *J Phys Conf Ser.* 2018 ;1032.
4. Thongpool V, Asanithi P, Limsuwan P. Synthesis of carbon particles using laser ablation in ethanol. *Procedia Eng.* 2012; 32: 1054–1060.
5. Yogesh G K, Shuaib E P, Kalai P A, Rohini P, Anandhan S V K, Uma Maheswari K V, et al..Synthesis of water-soluble fluorescent carbon nanoparticles (CNPs) from nanosecond pulsed laser ablation in ethanol. *Opt Laser Technol.* 2021; 135: 106717 .
6. Al-Jumaili B E B, Talib Z A, Zakaria A, Ramizy A, Ahmed N M Paiman, Suriati B, et.al.Impact of ablation time on Cu oxide nanoparticle green synthesis via pulsed laser ablation in liquid media. *Appl Phys A Mater Sci Process.* 2018 ; 124: 6.
7. Dizajghorbani A, Azadi H, Esmaeilzadeh M, Moemen Bellah S, Malekfar R. Ablation time and laser fluence impacts on the composition, morphology and optical properties of copper oxide nanoparticles. *Opt Mater. (Amst).* 2019; 91: 433–438.
8. Zhang W, Dai D, Chen X, Guo X, Fan J. Red shift in the photoluminescence of colloidal carbon quantum dots induced by photon reabsorption. *Appl Phys Lett.* 2014; 104.
9. Sadeghi H, Dorrnian D. Influence of size and morphology on the optical properties of carbon nanostructures. *J Theor Appl Phys.* 2016; 10: 7–13.
10. Altuwirqi R M, Albakri A S, Al-Jawhari H Ganash E A. Green synthesis of copper oxide nanoparticles by pulsed laser ablation in spinach leaves extract. *Optik (Stuttg).* 2020; 219: 165280.

11. Dorrnanian D, Eskandari A F. Effect of Laser Fluence on the Characteristics of ZnO Nanoparticles Produced by Laser Ablation in Acetone. *Mol Cryst Liq Cryst*. 2015; 607: 1–12.
12. Hoang V C, Hassan M, Gomes V G. Coal derived carbon nanomaterials – Recent advances in synthesis and applications. *Appl Mater Today*. 2018; 12: 342–358.
13. Małolepszy A, Błonski S, Chrzanowska-Giżyńska J, Wojasiński M, Płocinski T, Stobinski L, et al. Fluorescent carbon and graphene oxide nanoparticles synthesized by the laser ablation in liquid. *Appl Phys A Mater Sci Process*. 2018; 124: 1–7.
14. Tabatabaie N, Dorrnanian D. Effect of fluence on carbon nanostructures produced by laser ablation in liquid nitrogen. *Appl Phys A Mater Sci Process*. 2016; 122: 1–9.
15. Ganash E A, Al-Jabarti G A, Altuwirqi R M. The synthesis of carbon-based nanomaterials by pulsed laser ablation in water. *Mater Res Express*. 2020; 7.
16. Xiao J, Liu P, Wang C X, Yang G W. External field-assisted laser ablation in liquid: An efficient strategy for nanocrystal synthesis and nanostructure assembly. *Prog Mater Sci*. 2017; 87: 140–220.
17. Liu Z, Ling, Qian Cai Y, Xu L, Su J, Yu Kuai, Wu X, Xu J, et al. Synthesis of carbon-based nanomaterials and their application in pollution management. *Nanoscale Adv*. 2022; 4, 1246–1262.
18. Tajdidzadeh M, Zakaria Azmi T, Zainal A N, Ali K, Mohammed B, Goumri S, et al. Improving stability of zinc nanoparticles in chitosan solution with a nanosecond pulsed laser. *Laser Phys Lett*. 2019; 16.
19. Rashed H H, Fadhil F A, Hadi I H. Preparation and characterization of lead oxide nanoparticles by laser ablation as antibacterial agent. *Baghdad Sci J*. 2017; 14(4): 801- 807.
20. Fawadi E M, Al -Alwan N, Tariq J, Naji I S. The Structure and Optical properties of CdSe: Cu Thin Films. *Baghdad Sci J*. 2009; 6 (1): 1-9.
21. Sun Y P, Zhou B, Lin Y, Wang W, Fernando K A S, Pathak P, Meziani M J, et al. Quantum- sized carbon dots for bright and colorful photoluminescence. *J Am Chem Soc*. 2006; 128: 7756–7757.
22. Zheng H, Wang Q, Long Y, Zhang H, Huang X, Zhu Rui. Enhancing the luminescence of carbon dots with a reduction pathway. *Chem Commun*. 2011; 47: 10650–10652.
23. Hu S, Dong Y, Yang J, Liu J, Cao S. Simultaneous synthesis of luminescent carbon nanoparticles and carbon nanocages by laser ablation of carbon black suspension and their optical limiting properties. *J Mater Chem*. 2012; 22: 1957–1961.
24. Masha S, Oluwafemi O S. Synthesis of blue and green emitting carbon-based quantum dots (CBQDs) and their cell viability against colon and bladder cancer cell lines. *Mater Lett*. 2021; 283: 128790.
25. Alaghmandfard A, Sedighi Omid, Tabatabaie R N, Abedini A A, Malek Kh A, Toprak M S, et al. Recent advances in the modification of carbon-based quantum dots for biomedical applications. *Mater Sci Eng C*. 2021; 120, 111756.

تأثير سرعة القشط على تخليق مركبات كربونية بواسطة القشط الليزري النبضي للإسفلت بالإيثانول

مهند موسى عزوي²

هدى محمود العطار¹

¹ كلية الهندسة، جامعة بغداد، العراق.

² مركز بحوث الليزر والكهربويات، وزارة العلوم والتكنولوجيا، العراق

الخلاصة:

القشط الليزري بالسائل يعتبر كطريقة خضراء لتخليق الملايكات النانوية وذلك بسبب عدم وجود ناتج جانبي بالإضافة الى الناتج الاصيلي بعد القشط الليزري في هذا البحث فايبر ليزر بطول موجي $1.064 \mu\text{m}$ ، وبقيمة طاقة 1 mJ ، بزمان نبضي 120 ns ، وبتردد تكرار للنبضة 20 kHz استخدم لتخليق المركبات النانوية. المحلول النانوي المخلوق يتضمن كرات نانوية كربونية وقضائيب نانوية كربونية نتجت من قشط الاسفلت بالإيثانول وبسرعة قشط $(100, 75, 50, 10 \text{ mm/s})$. المورفولوجيا، التركيب والخواص البصرية للنماذج المخلقة درست مختبرياً بواسطة FESEM, HRTEM, EDS ومطياف الاشعة فوق البنفسجية والمرئية. أظهرت النتائج بأن فجوة الطاقة نقل بنقصان سرعة القشط (زيادة وقت القشط) أقل معدل حجم حبيبي للنماذج المخلقة كان 76 nm وبسرعة قشط 100 mm/s ، بينما كان أقصى معدل للحجم الحبيبي هو 98 nm عند سرعة قشط 50 mm/s لوحظ تكثر الكرات النانوية لتكوين اشكال نانوية أكبر. كل المحاليل النانوية الكربونية اعطت طيف انبعاث فلورة في الطول الموجي الاخضر المزرق. نستنتج بأن وجود القضائيب النانوية كان له تأثير على الخواص البصرية للكريات النانوية المخلقة.

الكلمات المفتاحية: القضبان الكربونية النانوية، الكريات الكربونية النانوية، فايبر ليزر $1.06 \mu\text{m}$ ، الفلورة، القشط الليزري النبضي.